Statistical Similarities Between WSA-ENLIL+Cone Model and MAVEN in situ Observations from November 2014 to March 2016.

C. L. Lentz[1] , D. N. Baker[1], A. N. Jaynes[1], R. M. Dewey[3], C. O. Lee[5], D. A. Brain[1], J. S. Halekas[4]

[1] Laboratory for Atmospheric and Space Physics, University of Colorado, Boulder, CO, USA.
[2] Catholic University of America, Washington, DC, USA.
[3] Department of Climate and Space Sciences and Engineering, University of Michigan, Ann Arbor, MI, USA.
[4] Department of Physics and Astronomy, University of Iowa, Iowa City, Iowa, USA.
[5] Space Sciences Laboratory, University of California, Berkeley, CA, USA.

Corresponding Author: Christy.lentz@lasp.colorado.edu

Abstract:

Normal solar wind flows and intense solar transient events interact directly with the upper Martian atmosphere due to the absence of an intrinsic global planetary magnetic field. Since the launch of the Mars Atmosphere and Volatile EvolutioN (MAVEN) mission, there is now a means to directly observe solar wind parameters at the planet's orbital location for limited time spans. Due to the craft's highly elliptical orbit, in situ measurements cannot be taken while MAVEN is inside Mars' magnetosheath. In an attempt to model solar wind conditions during these atmospheric and magnetospheric passages, this research project utilizes the solar wind forecasting capabilities of the Wang-Sheeley-Arge-ENLIL+Cone (WEC) model. These sets of tools are maintained at the Community Coordinated Modeling Center (CCMC). In this study, the model has simulated solar wind parameters such as plasma pressure, temperature, particle density, velocity and magnetic field properties during the time period from December 2015 to March of 2016, with an additional extended simulation from late November 2014 to March 2016. The accuracy of the model was examined for intervals when MAVEN was considered to be in upstream solar wind,

i.e., with no exospheric or magnetospheric phenomena altering the in situ measurements. It was determined that the WEC model has the capability to provide statistically similar baseline values for continuous solar wind knowledge. These baseline values can be further improved upon in accuracy when smaller time scales (e.g. 1-2 Carrington rotations) are analyzed. Generally, this study aims to provide a larger context of solar wind driving during gaps in the in situ measurements.

1. Introduction

With the insertion of MAVEN into Mars' orbit on 21 September 2014 (Jakosky et al., 2014) new data coming in are being pored over as MAVEN provides first-hand observations of the long-term effects of solar transient events on Mars' atmosphere. This provides insight regarding the evolution of the planetary atmosphere. In an attempt to model solar wind conditions during the MAVEN mission, the WSA-ENLIL+Cone (WEC) model was used for the time period of December 2015 to March 2016, and then a separate run that captured solar wind trends from late November 2014 to March of 2016 [Arge and Pizzo, 2000, Odstrčil, 2004, Xie et al., 2004]. We report here on the accuracy of the WEC model's predictions of solar wind parameters such as velocity of the plasma, particle density, pressure, temperature and interplanetary magnetic field strength from the two separate runs. With extensive analysis of the WEC model's performance, there is a possibility of using the model values for times when MAVEN is unable to obtain in situ measurements during deep-dip campaigns. The aim of this study was to take predictions from the WEC model for the first detailed run and compare them to the orbit-averaged in situ measurements to check for statistical similarities. Then to take the second extended time period and determine if its results were at all comparable to the detailed run. The goal is to use extended runs to provide continuous solar wind forcing knowledge even if they do not contain all documented solar transient events. From this we can therefore have a continuous record of solar wind forecasting around Mars' orbital location.

2. Background

2.1 The MAVEN Mission

MAVEN is in a highly elliptical orbit with a low altitude periapsis of ~150 km, that allows it to enter and exit the magnetic pileup boundary (MPB) and the bow shock (BS) once every orbit, regardless of the boundary altitudes changes [see Edberg et al., 2009]. MAVEN therefore can measure the solar and solar-wind energetic input into the upper atmosphere [e.g., Jakosky et al., 2015]. Compared to the other missions to study Mars' atmosphere, MAVEN provides the most comprehensive measurements that are essential to the understanding of the time evolution of the Martian atmosphere. For example, the Mars Global Surveyor (MGS) which orbited Mars for ten years (losing signal in November of 2006, "Mars Global Surveyor") had instruments on board that were never designed to observe such phenomena as Interplanetary Coronal Mass Ejections (ICME) and Solar Energetic Particles (SEP) [Falkenberg et al., 2001]. Another recent European mission, the Mars Express (MEX), has a different scientific focus and therefore does not include a magnetometer and only has atmospheric/ionospheric instruments such as the Energetic Neutral Ion analyzer [Barabash et al., 2006]. MAVEN, on the other hand, includes a complete set of atmosphere-measuring and contextual instruments such as the Solar Wind Electron Analyzer [Mitchell et al., 2015] and the Solar Wind Ion Analyzer [Halekas et al., 2013]. However, as MAVEN ascends or descends into the bowshock and other layering regions, there are time periods when there is no method to extract data on solar wind parameters such as the velocity of the plasma, particle density, pressure, temperature and magnetic field properties. This is where solar wind forecasting models can be utilized to predict supplemental solar wind parameter values [e.g. Dewey et al., 2017].

2.2 WSA-ENLIL+Cone (WEC) Background

Among the numerous (38) space weather models that the Community Coordinated Modeling Center (CCMC) has to offer, the semi-empirical near-Sun Wang-Sheeley-Arge [Arge and Pizzo, 2000; Arge et al., 2004] model coupled with the three-dimensional magnetohydrodynamic numerical model, ENLIL (Enlilv2.8f) [Odstrčil, 2003] combined with the Cone model [Xie et al., 2003] provide information that is needed to describe the propagation of a CME from the Sun's photosphere to Mars' orbital location. This combination of models, along

with only WSA-ENLIL, has been used in other planetary interaction studies such as at Mercury [e.g., Baker et al., 2009, 2010, 2013 and Dewey et al., 2015].

Going into detail, the WSA model contrives predictions of solar wind speed and interplanetary magnetic field (IMF) strength by using ground-based observations of the solar surface magnetic field as input to a magnetostatic potential-field source surface (PFSS) model [Schatten et al., 1969]. The WSA model then provides boundary conditions at 21.5 Solar Radii that can be given to ENLIL to subsequently model the solar wind flow outward to distances further than 1 AU [Odstrcil et al., 2004b]. Along with the WSA model input, ENLIL can also take the Cone model's input parameters. These input parameters provide distinctive CME specifications such as the width, orientation and registered speed of each particular CME. The Cone model is a vital addition to the WSA-ENLIL combination because it assumes that CMEs propagating from the Sun do so with constant angular and radial velocity therefore form a cone shape, thus simulating a more realistic CME propagation. The three models therefore provide state-of-the-art forecasts of solar wind flow speed, plasma density, solar wind mean plasma temperature, and magnetic field strength throughout the inner heliosphere.

To acquire a simulation run, a list of CMEs must be provided along with a source for solar magnetograms. For the initial detailed period of this study (late December 2015 to March 2016), along with the second period of study (November 2014 to March 2016), a list of CMEs was obtained from the Database Of Notifications, Knowledge, Information (DONKI) space weather activity archive (kauai.ccmc.gsfc.nasa.gov/DONKI/).The database, which contains a catalog of numerous types of solar activity, is a result of the NASA Space Weather Research Center (SWRC) team daily monitoring of the space environment for NASA's science campaigns. Although there are some caveats with the system due to measurements being subject to human error [e.g., Millward et al., 2013] all events occurring after August 2013 are said to be carefully reviewed by CCMC staff [Mays, 2016]. The CCMC continuously updates a list of derived CME geometries that are obtained from spacecraft that are observing a CME event near the solar limb similar to the process described in Lee et al. [2012].

The synoptic solar magnetograms chosen for this study were selected from the National Solar Observatory's Global Oscillation Network Group (GONG) [Harvey et al., 1996]. GONG's magnetograms were chosen due to their high cadence. GONG remaps minute-by-minute images to get a weighted sum to form a full-surface map of the photospheric magnetic flux density

(gong.nso.edu). However, it is noted on the model-run request site that GONG data have known issues with the polar fields, which are being studied by the GONG staff (ccmc.gsfc.nasa.gov).

It should also be mentioned that the WEC model's CME arrival times are reliant upon the initial CME geometry input parameters [Mays et al., 2015]. Accuracy has also been shown by Lee et al., (2012) to be reliant on the initial precision of the modeled background solar wind, which is determined by the input solar magnetograms supplied by the GONG observatories. In comparable studies, the most favorable magnetograms are ones that are updated on a 24-hour cadence to provide the utmost complete global photosphere magnetic field map.

3. Data Observations and Analyses

3.1 Analysis of detailed run from December 2015 to March 2016

This study expands on previous techniques to determine solar wind conditions at Mars by modeling solar wind conditions from the solar surface to Mars' orbital location [REF]. We compared the results from the WSA-ENLIL+Cone (WEC) model with direct solar wind and IMF measurements from the MAVEN spacecraft over the period from December 2015 to March 2016. In this period of study, there were a total of 83 CMEs documented on the DONKI database. All of these were used in the run and Figure 1 shows the results of the detailed run.

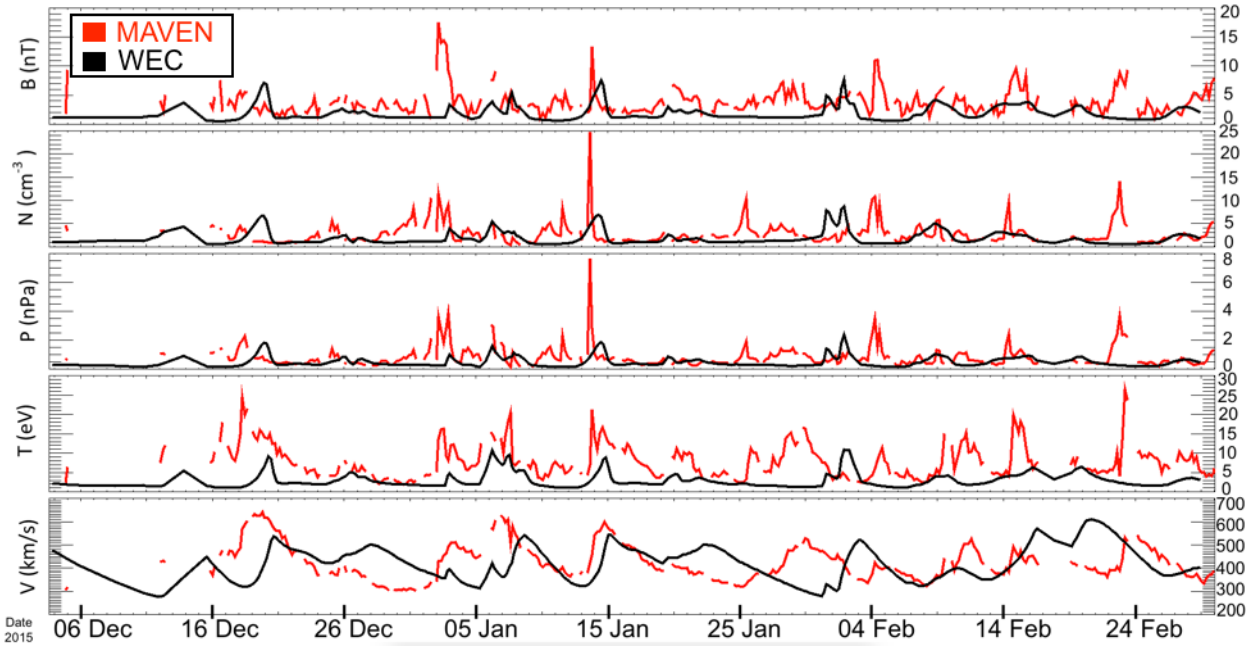

Figure 1: The WEC model results for the period December 2015 through March 2016. WEC

(black) computed values and MAVEN (red) actual observations of IMF B, and solar wind parameters N, P, T and V are shown from the first to the fifth panel, respectively. Note the sparsity of data for MAVEN at the beginning of this time period is due to MAVEN not being in an interval of pristine solar wind.

In order to analyze the accuracy of the WEC model compared to MAVEN observations we first found how much or how little the modeled distribution underestimates or overestimates each solar wind parameter. To visualize this, Figure 2 includes histograms of the frequency distributions. It can be seen that solar wind speed is one of the best represented parameters. Taking everything into account, the WEC model tends to have smaller spreads than MAVEN's actual observations.

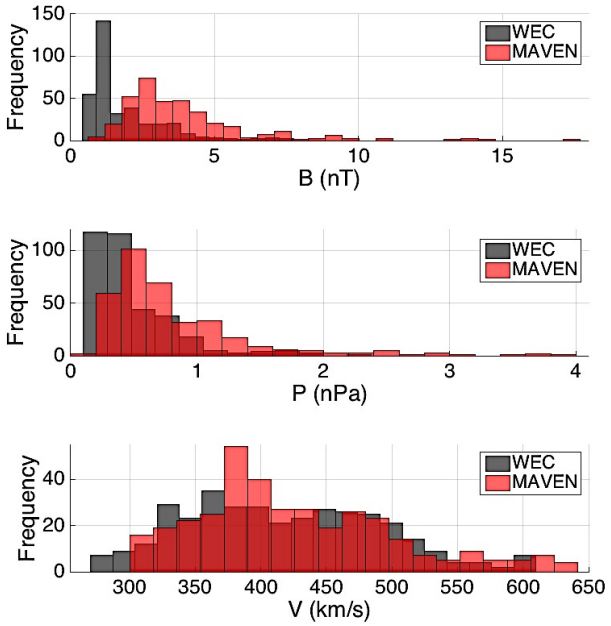

Figure 2: Histograms of frequency distributions from the entire detailed run from December 2015 to March 2016. Where the model's data have been orbit-averaged in order to compare to MAVEN's orbit averaged data sets. the bin sizes were chosen specifically for each parameter in order to adequately represent the data density

To aid in the visualization of the WEC model and MAVEN solar wind parameter comparisons, we have also included a series of "box plots" with a brief explanation of what each plot element means in the lower right corner. The box plots help to demonstrate the performance of the ENLIL component of WEC. ENLIL, which is a numerical code for solar wind disturbances, is responsible for the output of the five main solar wind parameters examined in this paper after receiving CME parameter information from the WSA and Cone model. In the following box plots,

the model's strengths in estimating solar wind speed can be easily seen. It can also be seen that the mean plasma temperature is under-predicted for the time period, as was found by Dewey et al., (2016). It is also clear that the WEC model continuously under predicts IMF strength, as stated by Dewey et al. [2015]. This can be attributed to the WEC model not including the magnetic cloud in simulation, [see Falkenberg et al., 2011]. Figure 3 aids in the visualization of the under-prediction of IMF strength.

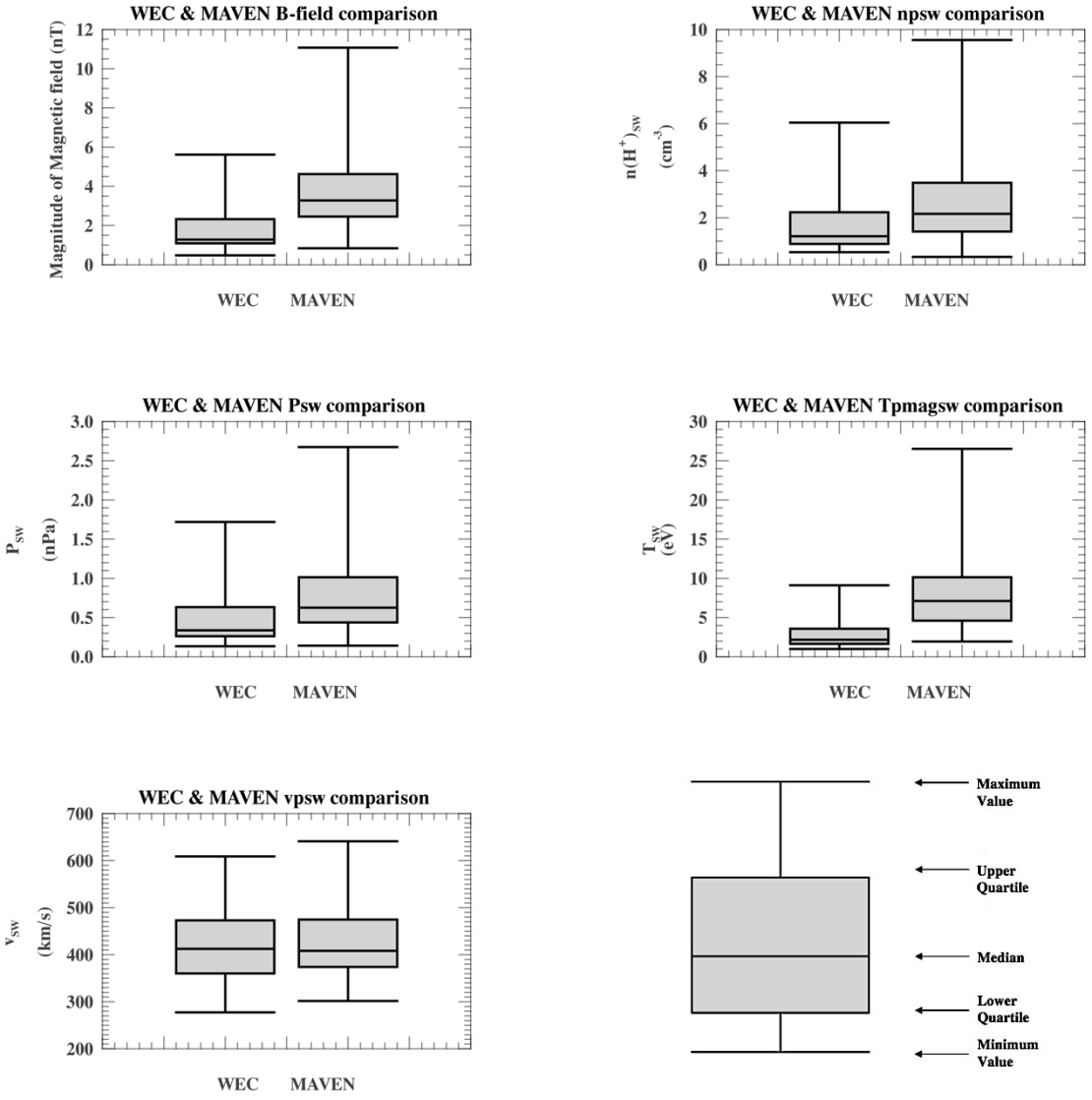

Figure 3: Box plots displaying maxima, minima, medians, upper and lower quartiles showing performance for WEC during December 2015 to March 2016

Probing the WEC data set further for this time period, Figure 4 shows the number of times local maxima were found that reach above specific thresholds. On average, WEC captured only half of the maxima that MAVEN measured for each of the five parameters.

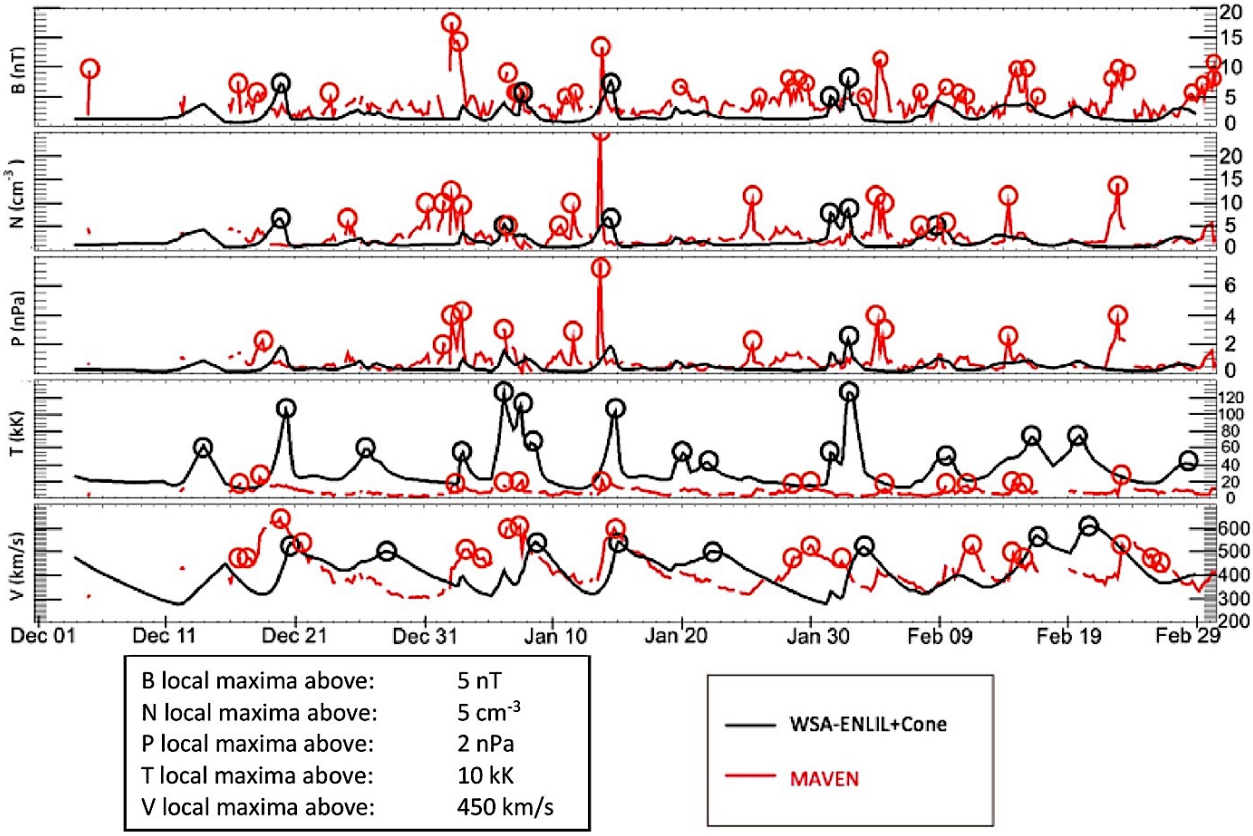

Figure 4: Maxima shown for each solar wind parameter during December 2015 to March 2016 that reach above specified values

To summarize the over/under-estimates of the WEC model compared to MAVEN, it was found that the IMF strength measured by MAVEN is on average 2.92 times more than WEC's estimated values. The proton density of MAVEN, as measured by the Solar Wind Ion Analyzer (SWIA) [J.S. Halekas et al., 2017], is 2.54 times more than the corresponding WEC values. Dynamic pressure values recorded by MAVEN were 2.59 times more than WEC's. The temperature of protons in eV of MAVEN was a factor of 3.63 times more than WEC's estimated values. Finally, MAVEN's recorded radial velocity of protons was 1.06 times more than WEC. Minima and maxima can also be visualized in the box plots of Figure 3.

To compare how well the model does at recovering solar wind transient features, the CME shock arrival times that MAVEN observed are plotted in Figure 5, along with the modeled and in situ wind parameters. These shock arrival times came from Lee et al. (2017) findings, where solar wind transient and energetic particle events as observed by MAVEN were documented. As defined in Falkenberg et al., (2011) a shock at Mars is a simultaneous jump in the pressure proxy of at least 2 nPa.

Figure 5: Identified CME shock arrival times depicted in light green from December 2015 to late March 2016 along with both MAVEN (red) and WEC (black)

To evaluate the accuracy of shock detection, we compare the peak dynamic pressure between WEC and MAVEN. For this time period, the first CME that impacted Mars was on 01-02-2016/03:50:00 UT. The peak dynamic pressure value was recorded to be 3.4 nPa. The second CME shock arrival time was recorded to be on 01-06-2016/02:40:00 UT measuring 3.0 nPa. the last impacting CME for this time range was on 02-04-2016/06:05:00 UT and the peak dynamic pressure was recorded at 3.3 nPa.

Referencing the WEC dynamic pressure data set, WEC estimated the dynamic pressure on the 01-02-2016/03:50:00 UT CME to be 0.25 nPa, 01-06-2016/02:40:00 UT at 1.59 nPa and finally, 02-04-2016/06:05:00 UT at 0.22 nPa. Therefore, WEC underestimated the peak dynamic

pressure on average throughout this period by a factor of around 10 nPa. It should be noted for this period of detailed analysis that there are many apparent shocks in pressure which are missed by the simulation. The largest shock event, which occurred on 2016-01-13/15:00:00 UT measuring 7.59 nPa by MAVEN was missed by the WEC model. The closest event that the WEC model recorded was 2016-01-14/12:40:00 UT at 1.97 nPa.

3.2 Comparison between WEC model simulation results and MAVEN data for an extended time range.

in order to determine if the WSA-ENLIL+Cone (WEC) model could be used to obtain continuous solar wind forcing knowledge for an extended period of time, we performed a run for an extended period of time from November 2014 to March 2016. The simulation of the propagation, evolution and interaction of solar wind disturbances enroute to Mars is a challenging task and for such a lengthy stretch of time, it was beyond the capabilities of the simulation to include the total number of CMEs that occurred in the inner boundary file for ENLIL. However, it was still important to request this year-long run so that the model's capabilities and limitations can be further explored. We therefore filtered out CMEs that were too slow or too narrow. For example, CMEs that were detected by the Sun Earth Connection Coronal Heliospheric Investigation (SECCHI: Howard et al., 2008) on board the Solar Terrestrial Relations Observatory (SETERO A/B: Kaiser et al., 2007) and Large Angle Spectrometric Coronagraph C2 or C3 on board Solar and Heliospheric Observatory (SOHO: Domingo and Poland, 1995) that were detected to be under 300 km/s were excluded along with CMEs that had a half width less than 10.0. Table 2 shows the number of CMEs that were included for the extended time period versus the total number of CMEs that were documented from the DONKI website. The large time range was broken down into 3 seasons in order to better be analyzed. The following figures (Fig 6, 7, and 8) show a broad

November 2014 -March 2015	June 2015 - October 2015	December 2015-March 2016
197 CMEs total	179 CMEs total	83 CMEs total
101 used in simulation	92 used in simulation	46 used in simulation

Table 1: number of CMEs that were included for extended run versus the total numbers of CMEs documented on DONKI

overview of the data obtained from the WSA-ENLIL+Cone simulation for each of the three seasons.

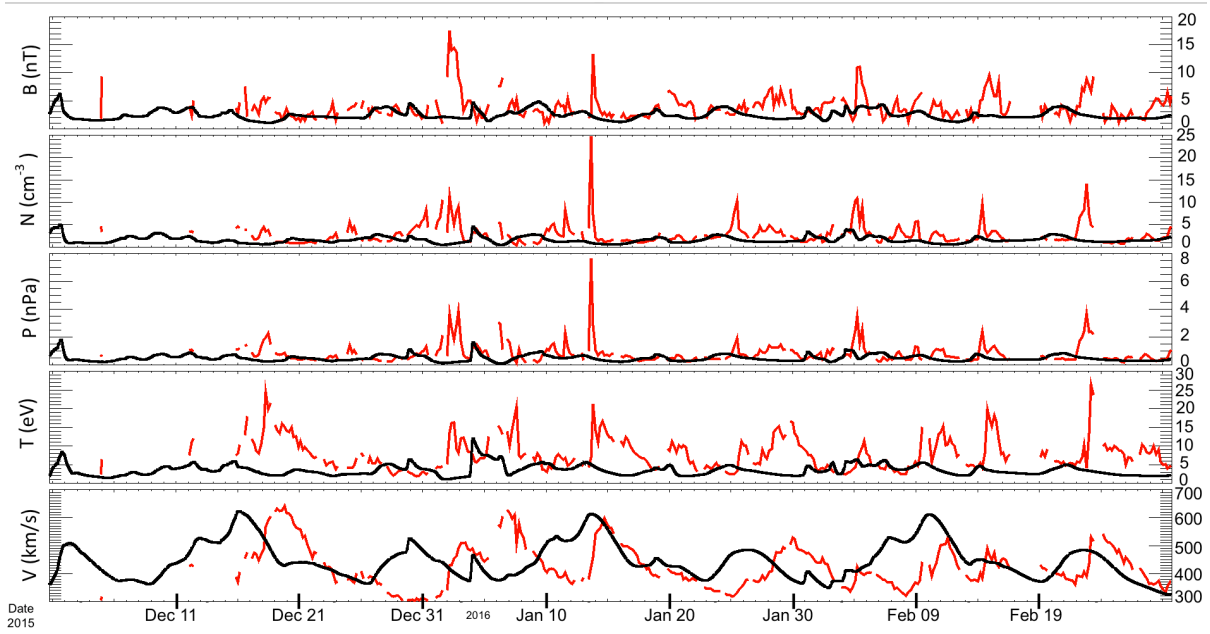

Figure 6: December 2015 to March 2016 season plotted for extended run. WEC (black) and MAVEN (red). The 5 solar wind parameters in each panel are as follows: magnitude of the magnetic field (B) measured in nT. The number of protons in solar wind (N) measured per cm^3. the RAM pressure (P) measured in nPa, the magnitude of temperature (T) measured in eV, and the velocity of protons (V) measured in km/s.

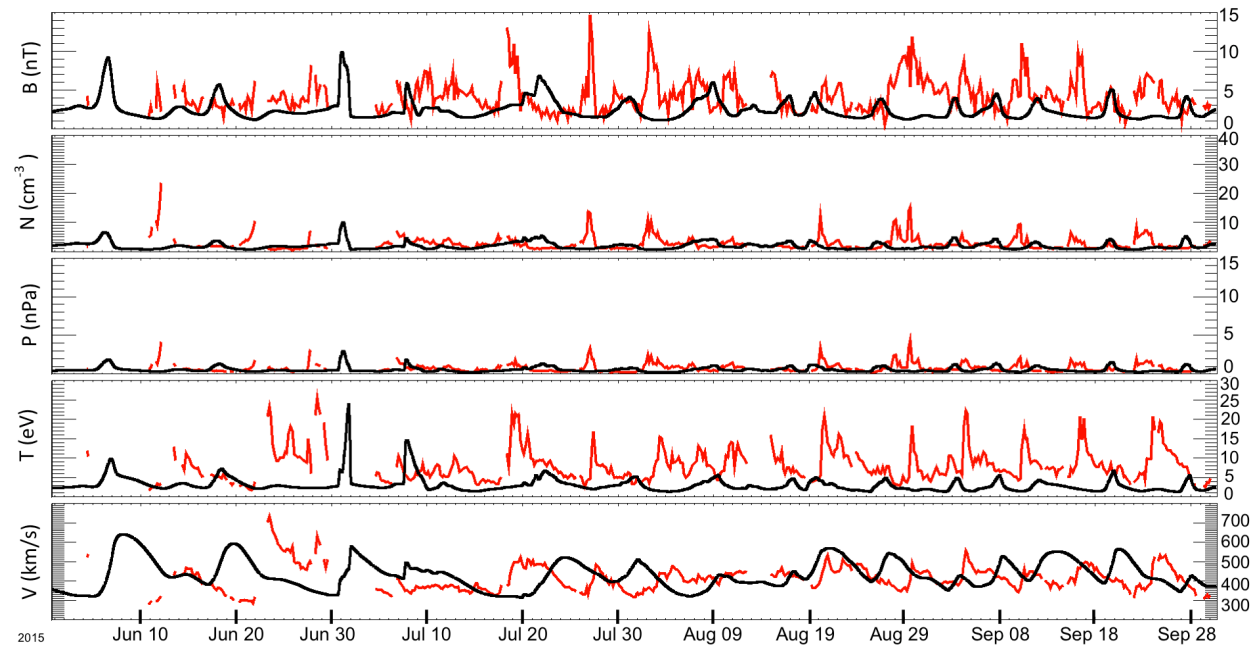

Figure 7: the preceding summer season June 2015 to October 2015. WEC (black) MAVEN (red).

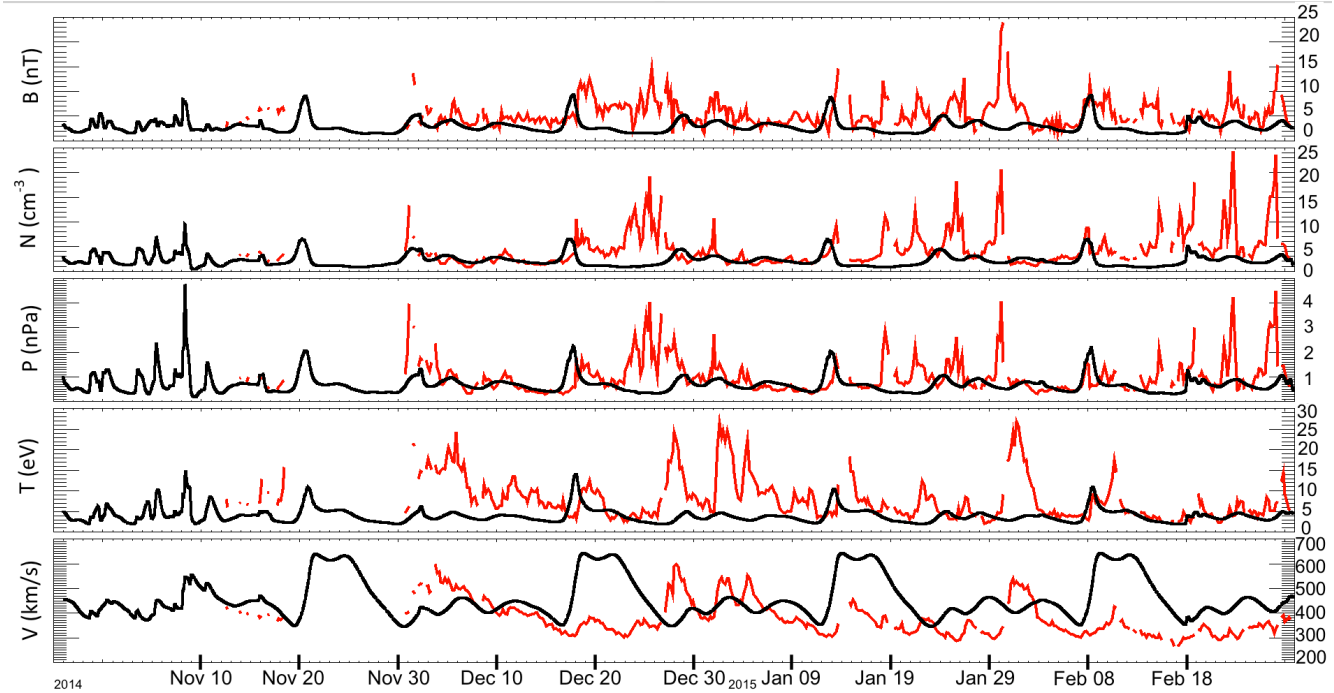

Figure 8: WEC (black) run from November 2014 to March 2015 MAVEN is depicted in red.

Upon inspecting all seasons to see if WEC model agreed with actual MAVEN observations, we conducted similar statistical analyses to the detailed run. It was found that for the extended (i.e. less detailed) run from December 2015 to March of 2016, the IMF strength measured by MAVEN was on average 1.78 times more than WEC's. MAVEN's proton density was on average 2.52 times more than WEC's, MAVEN's dynamic pressure was on average 2.35 times more than WEC's. MAVEN's temperature was 2.81 times more than WEC's estimate, and WEC's solar wind speed was on average 1.09 times more than MAVEN's SWIA instrument documented. When comparing MAVEN's temperature values to WEC estimated temperatures, it should be noted that temperature values from MAVEN for the orbited averaged data are overestimated, this is especially true for the coldest solar wind because temperature measurements are limited by the instrumental energy and angular resolution [J. Halekas, personal communication, 30 March 2017].

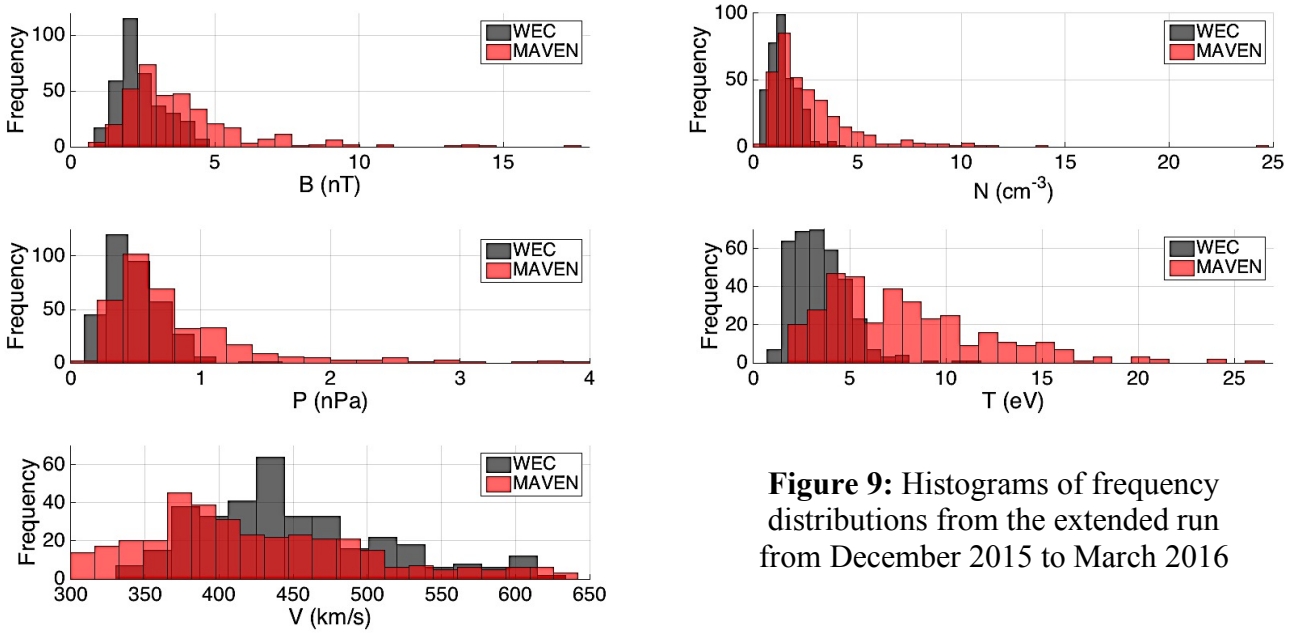

Figure 9: Histograms of frequency distributions from the extended run from December 2015 to March 2016

For the summer season, June 2015 to October 2015, it was found that the IMF strength measured by MAVEN was on average 2.21 times that of WEC's, WEC's proton density was 1.05 times that of MAVEN's. WEC's dynamic pressure was 1.03 times more than MAVEN's. MAVEN's mean plasma temperature estimates were found to be 3.55 times more than MAVEN's, and WEC's velocity was 1.08 times more than MAVEN's.

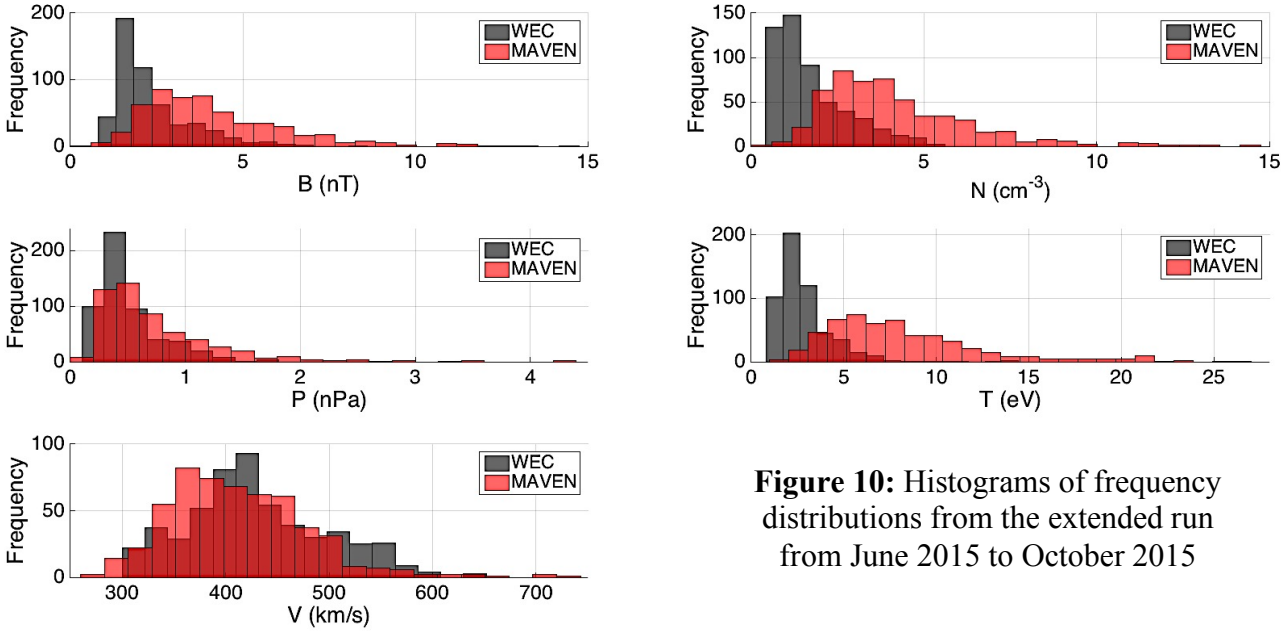

Figure 10: Histograms of frequency distributions from the extended run from June 2015 to October 2015

For the first winter season (i.e. November 2014 to March 2016) for the extended run, the IMF strength measured by MAVEN was on average 1.78 times more than WEC's. MAVEN's proton density was a factor of 2.74 more than WEC's. MAVEN's dynamic pressure was 1.75 times that of WEC's. MAVEN's temperature was a factor of 2.31 more than that of WEC's estimate. WEC's velocity is 1.17 times that of MAVEN's.

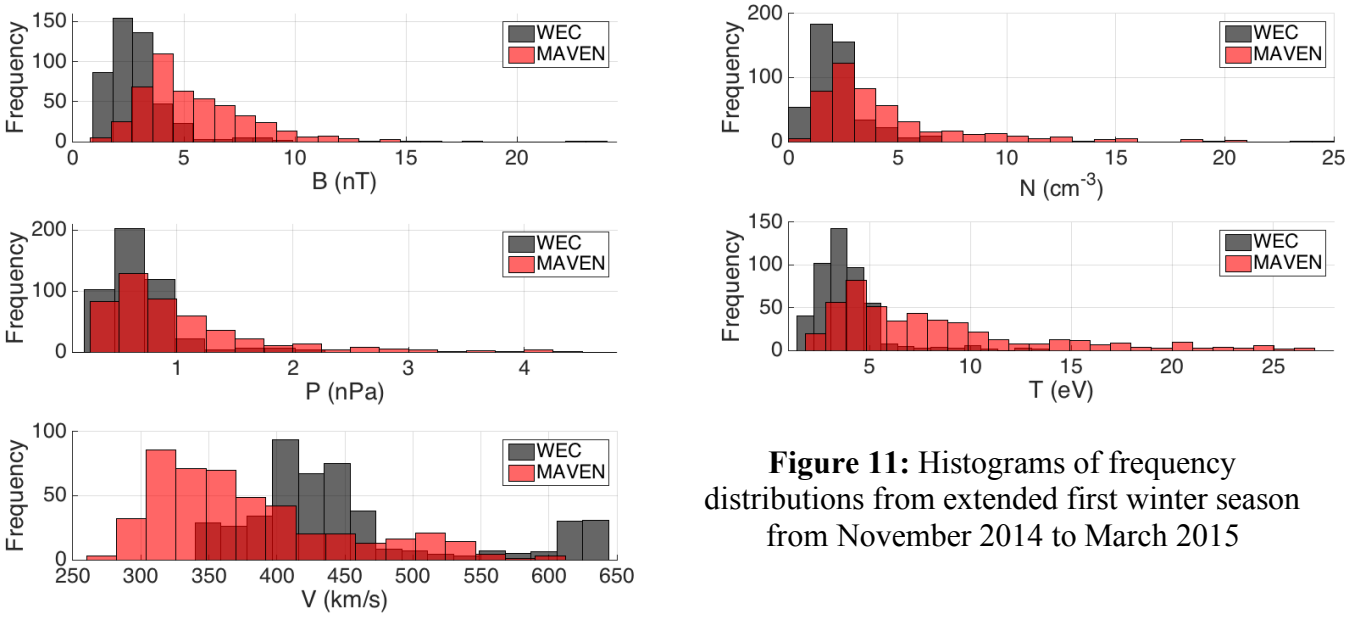

Figure 11: Histograms of frequency distributions from extended first winter season from November 2014 to March 2015

We then continued to probe the performance of the WEC model using the mean square error (MSE) as a measure of prediction accuracy. Averaging the three season's MSEs during the extended time period, it was found that the average MSE for IMF strength was 11.79 nT^2, and 10.11 nT^2 for the detailed run. The proton density (N) had a MSE of 11.50 cm^{-6} for the extended, 8.70 cm^{-6} for the detailed. The dynamic pressure (P) was 0.74 nPa^2 for the extended, 0.72 nPa^2 for the detailed. Proton temperature (T) MSE was calculated to be 50.79 eV^2 for the extended, 44.83 eV^2 for the detailed run. Finally, solar wind speed (V) MSE was

Time period	MSE B (nT^2)	MSE N (cm^{-6})	MSE P (nPa^2)	MSE T (kK^2)	MSE V (km^2/s^2)
November 2014-March 2015 (extended)	17.53	14.55	0.62	57.66	$1.59*10^4$
June 2015-October 2015 (extended)	10.03	11.96	0.88	50.88	$1.23*10^4$
December 2015-March 2016 (extended)	7.80	8.00	0.72	43.85	$1.07*10^4$
December 2015-March 2016 (detailed)	10.11	8.70	0.72	44.83	$1.21*10^4$

Table 2: Mean Square Error between WEC and MAVEN for each period of time.

285 found to be $1.3*10^4 \frac{km^2}{s^2}$ for the extended run compared to 1.21e04 $\frac{km^2}{s^2}$ for the detailed. These
286 results are summarized in Table 2, note that a value closer to 0 is preferable.
287
288 Continuing with the parameter
289 comparisons, we found the ratio of
290 median values modeled by WEC and
291 observed by various MAVEN
292 instruments for the detailed run and for
293 the extended run. Here values closer to 1
294 display excellent agreement between the
295 model and the observations. We see that
296 the averaged median ratio of the IMF
297 strength estimated by WEC compared to
298 MAVEN (B_{WEC}/B_{MAVEN}) for the extended run is 0.59 compared to the detailed run which was 0.39.
299 N_{WEC}/N_{MAVEN} averaged for the extended run was 0.63 and 0.56 for the detailed. P_{WEC}/P_{MAVEN}
300 averaged was 0.75 for the extended period compared to 0.54 for the detailed period. T_{WEC}/T_{MAVEN}
301 for the extended time period was 0.44 compared to 0.31 for the detailed period. V_{WEC}/V_{MAVEN} was
302 1.09 for the extended period and 1.01 for the detailed period. Table 3 summarizes these results
303 with the exception that the extended period is broken up into seasons.

Time Period	B_{WEC}/B_{MAVEN}	N_{WEC}/N_{MAVEN}	P_{WEC}/P_{MAVEN}	T_{WEC}/T_{MAVEN}	V_{WEC}/V_{MAVEN}
November 2014-March 2015 (extended)	0.55	0.60	0.82	0.54	1.17
June 2015- October 2015 (extended)	0.54	0.68	0.71	0.33	1.03
December 2015 – March 2016 (extended)	0.69	0.62	0.73	0.46	1.07
December 2015-March 2016 (detailed)	0.39	0.56	0.54	0.31	1.01

Table 3: Ratio of median values of WEC versus MAVEN for each time period.

304
305 Concluding our parameter comparison, we also conducted analysis on the shock arrival
306 times as observed by MAVEN from December 2014 to March 2016. The shock arrival times for
307 the extended run were also taken from Lee et al., (2017). In Figure 12, the first winter period is
308 plotted with identified shock arrival times at MAVEN's orbital location. The values are determined
309 from the orbit-averaged resolution upstream solar wind data set. During the winter period from
310 December 2015 to March 2016 for the extended run, MAVEN detected three total CMEs. The first
311 arriving on 01-02-16/03:50:00 UT measuring 3.4 nPa, and 01-06-16/02:40:00 UT measuring 3.0
312 nPa and then on 02-04-16/06:05:00 UT measuring 3.3. WEC's corresponding dynamic pressure
313 values were 0.16 nPa, 0.16 nPa and 0.87 nPa, respectively. Therefore, on average, WEC
314 underestimated peak dynamic pressure by a factor of ~15. Compared to the detailed period where

peak dynamic pressure was under predicted by a factor of ~10. Figure 12 displays the identified CME shock arrival times and MAVEN and WEC's corresponding parameters during these times.

Figure 12: Identified CME shock arrival times for the extended run depicted in light green from December 2015 to March 2016 where MAVEN is in red and the WEC model in black.

For the summer time period during the extended run, MAVEN recorded a CME shock arrival on 07-06-15/20:00:00 measuring 2.1 nPa and a second CME on 10-06-15/17:30:00 measuring 3.5 nPa. WEC's corresponding measurements during these time periods were 0.53 and 2.05 nPa, respectively. Therefore, under-predicting peak dynamic pressure by a factor of ~3.

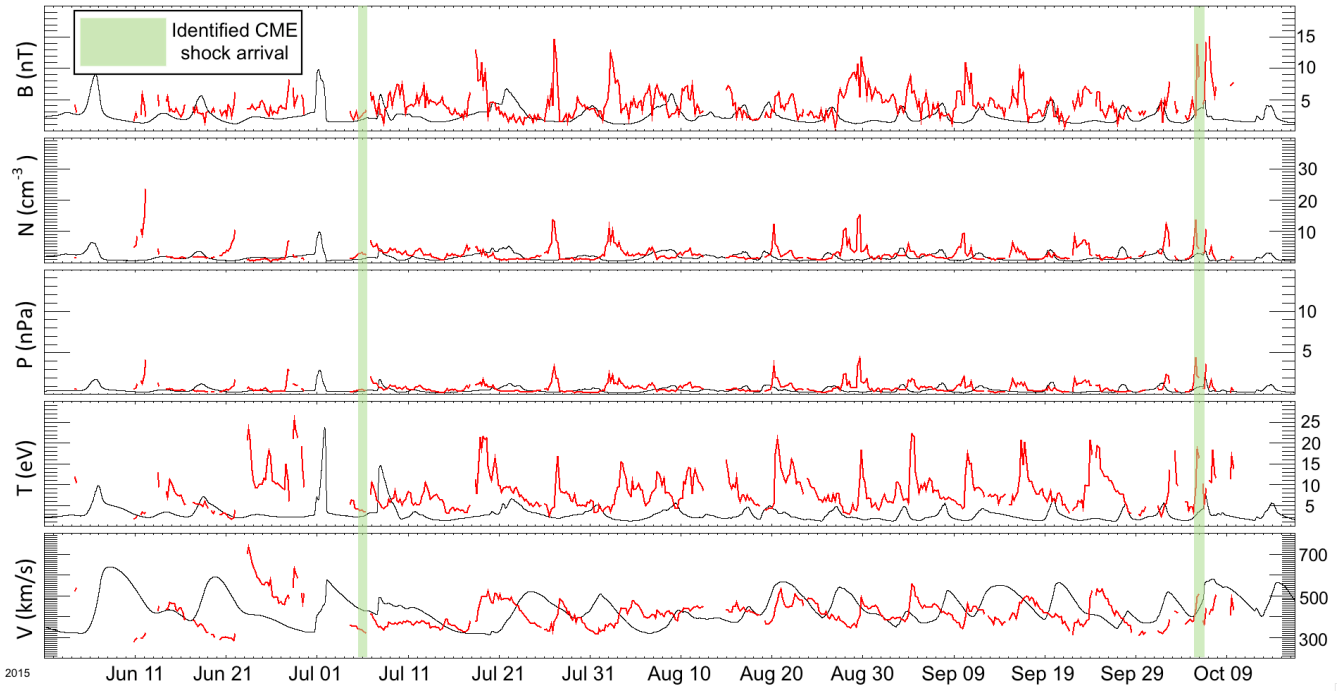

Figure 13: Identified CME shock arrival times for the extended run depicted in light green as observed by MAVEN from June 2015 to October 2015 where MAVEN is in red and the WEC model in black

During the first winter period from November 2014 to March 2015, there were a total of 5 CMEs that impacted Mars. MAVEN observed the first on 12-18-14/02:00:00 UT at measuring 1.6 nPa, 02-27-15/02:30:00 UT with 4.5 nPa, 03-04-15/04:40:00 with 6.5 nPa, 03-07-15/04:00:00 UT with 4.5 nPa and finally 03-08-15/21:00:00 UT measuring 12.5 nPa.

The corresponding simulated WEC values for these time periods were 1.91 nPa at 12-18-2014/02:00:00 UT, 0.69 nPa at 02-27-2015/02:30 UT, 5.97 nPa at 03-04-2015/04:40:00 UT, 1.38 nPa at 03-07-2015/04:00:00 UT, and 0.88 nPa at 03-08-2015/21:00:00 UT. WEC therefore under-predicted MAVEN observed peak dynamic pressure values by a factor of 5. Averaging the underestimations throughout the entire extended period of analysis, WEC under-predicted observations by a factor of 8. Compared to the detailed period of analysis which under-predicted the three documented CMEs by a factor of 10.

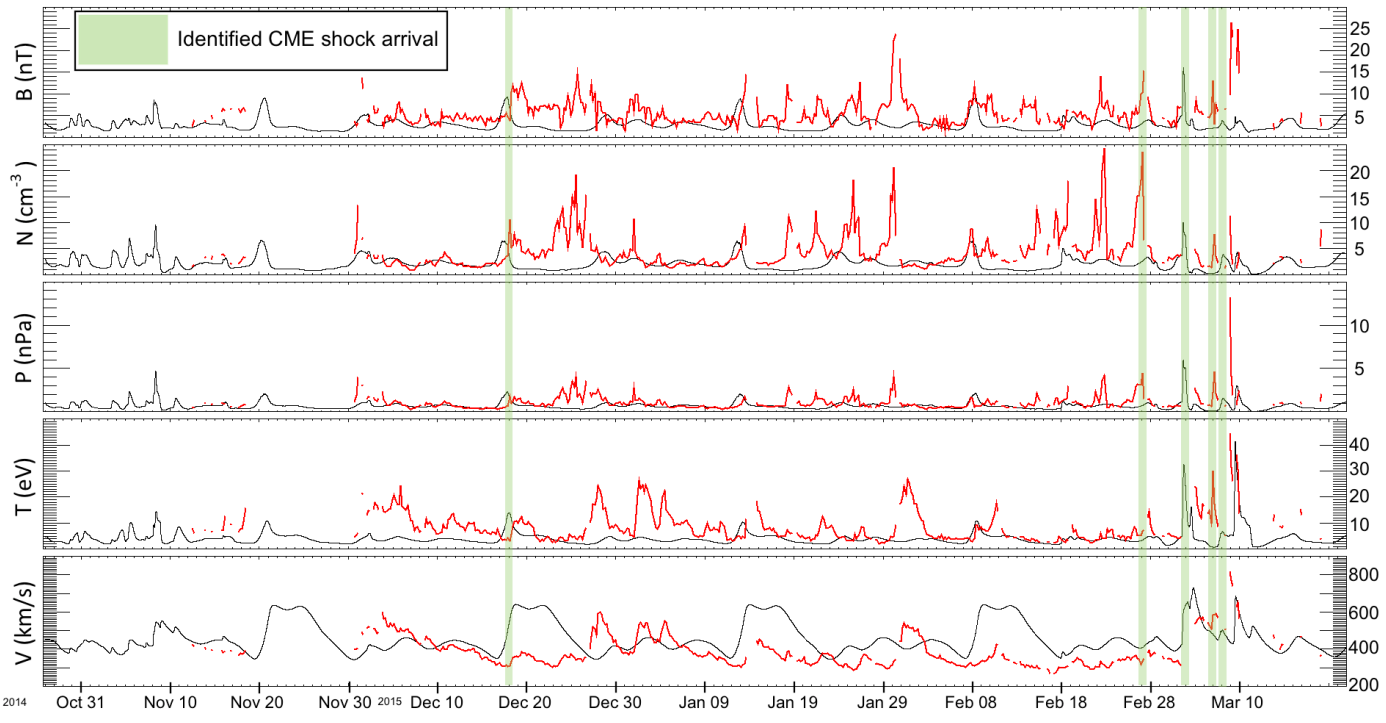

Figure 14: Identified CME shock arrival times for the extended run depicted in light green as observed by MAVEN from November 2014 to March 2015 where MAVEN is in red and the WEC model in black.

4. Discussion and Conclusion

Expanding on pre-existing methods that determine solar wind conditions at Mars, we first tested a detailed and relatively short time period (December 2015 to March 2016) to get an idea of the overall sensitivity of the model, and to determine the accuracy of the results. Then we requested an extended run from November 2014 to March 2016 to demonstrate that although not all CMEs were included in the simulation, it is still possible to have an average continuous account of solar wind conditions near Mars' orbital location. Whereas Dewey et al. (2017) compared background solar wind statistics at Mars to those at 1 AU from late November 2014 to mid-March 2015, along with the 8 March ICME case study, this study examined a wider time range, along with determining whether or not extended periods of analysis are as valid as shorter runs. The hope is

that with the use of the WEC model as a characterization tool, we can provide contextual information for planetary studies, especially for times where there is no means to obtain pristine solar wind readings.

It has been shown in multiple studies [e.g., Dewey et al., 2017, Lee et al., 2015, Dewey et al., 2015] that even in detailed runs, the WEC model does not completely capture trends of observed solar wind and IMF properties (e.g., under-prediction of IMF strength, systematic over prediction of temperature). As found by Falkenberg et al., [2011] many ICMEs change direction in propagation so assuming radial propagation from their point of origin may not be valid in all cases. Therefore, by executing a more generalized and expansive simulation *does not* result in less accurate correlations between the model and observations. We have shown this through comparing MSE values with MAVEN and the WEC model from a detailed run along with an extensive run, comparing by what factors WEC over- or under-predicts MAVEN values for both runs, and comparing the ratio of medians for both runs. Given the model's limitations, having extended runs do not differ greatly compared to detailed runs. This demonstrates that it is possible to use extended periods to capture general trends and baseline values in solar wind parameters and IMF properties.

The data provided by MAVEN allows us to continually adjust the solar wind and interplanetary magnetic field modeling for reliability and overall validity. Both the extended and detailed runs discrepancies with in situ observations most likely come from the WEC model not including microscopic processes.

We therefore conclude that the WEC model will not only provide an ever-clearer representation of corotating interaction regions, high speed solar wind streams and interplanetary magnetic field properties, but also help to fill gaps that exist in the record of in situ spacecraft observations. As different campaigns are launched in an effort to document and characterize solar wind conditions at Mars, models such as WEC can provide aid in the understanding and depiction of the Martian space environment.

Acknowledgements

The MAVEN project is supported by NASA through the Mars Exploration Program. All original MAVEN data reported in this paper is archived by the NASA Planetary Data System. C.L. Lentz thanks M.L. Mays for providing valuable input on the models and who also conducted all of the simulations. The modeling techniques described in this paper were originally developed under the auspices of the National Science Foundation's Center for Integrated Space Weather Modeling (CISM). Simulation results have been provided by the Community Coordinated Modeling Center at Goddard Space Flight Center through their public Runs on Request system (http://ccmc.gsfc.nasa.gov).

References:

- Arge, C. N., and V. J. Pizzo. "Improvement in the Prediction of Solar Wind Conditions Using Near-real Time Solar Magnetic Field Updates." *J. Geophys. Res. Journal of Geophysical Research: Space Physics* 105.A5 (2000): 10465-0479, DOI: 10.1029/1999JA000262

- Baker, Daniel N., Dusan Odstrcil, Brian J. Anderson, C. Nick Arge, Mehdi Benna, George Gloeckler, Jim M. Raines, David Schriver, James A. Slavin, Sean C. Solomon, Rosemary M. Killen, and Thomas H. Zurbuchen. "Space Environment of Mercury at the Time of the First MESSENGER Flyby: Solar Wind and Interplanetary Magnetic Field Modeling of Upstream Conditions." *Journal of Geophysical Research: Space Physics* 114.A10 (2009), doi:10.1029/2009JA014287

- Baker, Daniel N., Dusan Odstrcil, Brian J. Anderson, C. Nick Arge, Mehdi Benna, George Gloeckler, Haje Korth, Leslie R. Mayer, Jim M. Raines, David Schriver, James A. Slavin, Sean C. Solomon, Pavel M. TrÃ¡vnÃÄek, and Thomas H. Zurbuchen. "The Space Environment of Mercury at the times of the Second and Third MESSENGER Flybys." *Planetary and Space Science* 59.15 (2011): 2066-074, DOI: 10.1016/j.pss.2011.01.018

- Baker, Daniel N., Gangkai Poh, Dusan Odstrcil, C. Nick Arge, Mehdi Benna, Catherine L. Johnson, Haje Korth, Daniel J. Gershman, George C. Ho, William E. Mcclintock,

Timothy A. Cassidy, Aimee Merkel, Jim M. Raines, David Schriver, James A. Slavin, Sean C. Solomon, Pavel M. TrÃ¡vnÃ-Ä□ek, Reka M. Winslow, and Thomas H. Zurbuchen. "Solar Wind Forcing at Mercury: WSA-ENLIL Model Results." *Journal of Geophysical Research: Space Physics* 118.1 (2013): 45-57, doi:10.1029/2012JA018064

- Balogh, A., V. Bothmer, N. U. Crooker, R. J. Forsyth, G. Gloeckler, A. Hewish, M. Hilchenbach, R. Kallenbach, B. Klecker, J. A. Linker, E. Lucek, G. Mann, E. Marsch, A. Posner, I. G. Richardson, J. M. Schmidt, M. Scholer, Y.-M. Wang, R. F. Wimmer-Schweingruber, M. R. Aellig, P. Bochsler, S. Hefti, and Z. Mikić. "The Solar Origin of Corotating Interaction Regions and Their Formation in the Inner Heliosphere." *Space Sciences Series of ISSI Corotating Interaction Regions* (1999): 141-78. Web.

- Connerney, J. E. P., J. Espley, P. Lawton, S. Murphy, J. Odom, R. Oliversen, and D. Sheppard. "The MAVEN Magnetic Field Investigation." *Space Science Reviews Space Sci Rev* 195.1-4 (2015): 257-91. Web.

- Dewey, R. M., D. N. Baker, M. L. Mays, D. A. Brain, B. M. Jakosky, J. S. Halekas, J. E. P. Connerney, D. Odstrcil, J. G. Luhmann, and C. O. Lee. "Continuous Solar Wind Forcing Knowledge: Providing Continuous Conditions at Mars with the WSA-ENLIL Cone Model." *J. Geophys. Res. Space Physics Journal of Geophysical Research: Space Physics* 121.7 (2016): 6207-222, DOI: 10.1002/2015JA021941

- Domingo, V., B. Fleck, and A. I. Poland. "SOHO: The Solar and Heliospheric Observatory." *Space Science Reviews* 72.1-2 (1995): 81-84, DOI: 10.1007/BF00768758

- Edberg, N. J. T., D. A. Brain, M. Lester, S. W. H. Cowley, R. Modolo, M. Fränz, and S. Barabash. "Plasma Boundary Variability at Mars as Observed by Mars Global Surveyor and Mars Express." *Ann. Geophys. Annales Geophysicae* 27.9 (2009): 3537-550. Web.

- Emmons, D., A. Acebal, A. Pulkkinen, A. Taktakishvili, P. Macneice, and D. Odstrcil. "Ensemble Forecasting of Coronal Mass Ejections Using the WSA-ENLIL with CONED Model." *Space Weather* 11.3 (2013): 95-106. Web.

- Falkenberg, T. V., A. Taktakishvili, A. Pulkkinen, S. Vennerstrom, D. Odstrcil, D. Brain, G. Delory, and D. Mitchell. "Evaluating Predictions of ICME Arrival at Earth and Mars." *Space Weather* 9.9 (2011), DOI: 10.1029/2011SW000682

- Gosling, J. T., and V. J. Pizzo. "Formation and Evolution of Corotating Interaction Regions and Their Three Dimensional Structure." *Space Sciences Series of ISSI Corotating Interaction Regions* (1999): 21-52. Web.

- Gressl, C., A. M. Veronig, M. Temmer, D. Odstrčil, J. A. Linker, Z. Mikić, and P. Riley. "Comparative Study of MHD Modeling of the Background Solar Wind." *Solar Physics Sol Phys* 289.5 (2013): 1783-801. Web.

- Halekas, J. S., S. Ruhunusiri, Y. Harada, G. Collinson, D. L. Mitchell, C. Mazelle, J. P. McFadden, J. E. P. Connerney, J. R. Espley, F. Eparvier, J. G. Luhmann, and B. M. Jakosky. "Structure, Dynamics, and Seasonal Variability of the Mars-solar Wind Interaction: MAVEN Solar Wind Ion Analyzer In-flight Performance and Science Results." *Journal of Geophysical Research: Space Physics*. N.p., 23 Jan. 2017. Web. 27 Feb. 2017.
- Howard, R. A., J. D. Moses, A. Vourlidas, J. S. Newmark, D. G. Socker, S. P. Plunkett, C. M. Korendyke, J. W. Cook, A. Hurley, J. M. Davila, W. T. Thompson, O. C. St Cyr, E. Mentzell, K. Mehalick, J. R. Lemen, J. P. Wuelser, D. W. Duncan, T. D. Tarbell, C. J. Wolfson, A. Moore, R. A. Harrison, N. R. Waltham, J. Lang, C. J. Davis, C. J. Eyles, H. Mapson-Menard, G. M. Simnett, J. P. Halain, J. M. Defise, E. Mazy, P. Rochus, R. Mercier, M. F. Ravet, F. Delmotte, F. Auchere, J. P. Delaboudiniere, V. Bothmer, W. Deutsch, D. Wang, N. Rich, S. Cooper, V. Stephens, G. Maahs, R. Baugh, D. Mcmullin, and T. Carter. "Sun Earth Connection Coronal and Heliospheric Investigation (SECCHI)." *Space Science Reviews* 136.1-4 (2008): 67-115. Web.

- Jakosky, B. M., J. M. Grebowsky, J. G. Luhmann, J. Connerney, F. Eparvier, R. Ergun, J. Halekas, D. Larson, P. Mahaffy, J. Mcfadden, D. L. Mitchell, N. Schneider, R. Zurek, S. Bougher, D. Brain, Y. J. Ma, C. Mazelle, L. Andersson, D. Andrews, D. Baird, D. Baker, J. M. Bell, M. Benna, M. Chaffin, P. Chamberlin, Y.- Y. Chaufray, J. Clarke, G. Collinson, M. Combi, F. Crary, T. Cravens, M. Crismani, S. Curry, D. Curtis, J. Deighan, G. Delory, R. Dewey, G. Dibraccio, C. Dong, Y. Dong, P. Dunn, M. Elrod, S. England, A. Eriksson, J. Espley, S. Evans, X. Fang, M. Fillingim, K. Fortier, C. M. Fowler, J. Fox, H. Groller, S. Guzewich, T. Hara, Y. Harada, G. Holsclaw, S. K. Jain, R. Jolitz, F. Leblanc, C. O. Lee, Y. Lee, F. Lefevre, R. Lillis, R. Livi, D. Lo, M. Mayyasi, W. Mcclintock, T. Mcenulty, R. Modolo, F. Montmessin, M. Morooka, A. Nagy, K. Olsen, W. Peterson, A. Rahmati, S. Ruhunusiri, C. T. Russell, S. Sakai, J.- A. Sauvaud, K. Seki, M. Steckiewicz, M. Stevens, A. I. F. Stewart, A. Stiepen, S. Stone, V. Tenishev, E. Thiemann, R. Tolson, D. Toublanc, M. Vogt, T. Weber, P. Withers, T. Woods, and R. Yelle. "MAVEN Observations of the Response of Mars to an Interplanetary Coronal Mass Ejection."*Science* 350.6261 (2015), DOI: 10.1126/science.aad0210

- Kahler, S. W., C. N. Arge, and D. A. Smith. "Using the WSA Model to Test the Parker Spiral Approximation for SEP Event Magnetic Connections." *Solar Physics Sol Phys* 291.6 (2016): 1829-852. Web.

- Kaiser, M. L., T. A. Kucera, J. M. Davila, O. C. St. Cyr, M. Guhathakurta, and E. Christian. "The STEREO Mission: An Introduction." *Space Science Reviews* 136.1-4 (2007): 5-16. Web.

- Lee, C. O., C. N. Arge, D. Odstrčil, G. Millward, V. Pizzo, J. M. Quinn, and C. J. Henney. "Ensemble Modeling of CME Propagation." *Solar Physics Sol Phys* 285.1-2 (2012): 349-68, DOI: 10.1007/s11207-012-9980-1

- Liewer, P. C., E. M. Dejong, J. R. Hall, R. A. Howard, W. T. Thompson, A. Thernisien, M. Maksimovic, K. Issautier, N. Meyer-Vernet, M. Moncuquet, and F. Pantellini. "Determination of CME Trajectories by Stereoscopic Analysis of STEREO/SECCHI Data." (2010): n. pag. Web.

- Mays, M. L., "Database of Notifications, Knoweldge and Information". *PDF* (2016): https://ccmc.gsfc.nasa.gov/RoR_WWW/SWREDI/2016/Mays_DONKI_201605.pdf

- Mays, M. L., A. Taktakishvili, A. Pulkkinen, P. J. Macneice, L. Rastätter, D. Odstrcil, L. K. Jian, I. G. Richardson, J. A. Lasota, Y. Zheng, and M. M. Kuznetsova. "Ensemble Modeling of CMEs Using the WSA–ENLIL Cone Model." *Solar Physics Sol Phys* 290.6 (2015): 1775-814. Web.

- Mays, M. L., B. J. Thompson, L. K. Jian, R. C. Colaninno, D. Odstrcil, C. Möstl, M. Temmer, N. P. Savani, G. Collinson, A. Taktakishvili, P. J. Macneice, and Y. Zheng. "Propagation Of The 2014 January 7 Cme And Resulting Geomagnetic Non-Event." *ApJ The Astrophysical Journal* 812.2 (2015): 145, DOI: 10.1007/s11207-015-0692-1

- Millward, G., D. Biesecker, V. Pizzo, and C. A. De Koning. "An Operational Software Tool for the Analysis of Coronagraph Images: Determining CME Parameters for Input into the WSA-Enlil Heliospheric Model." *Space Weather* 11.2 (2013): 57-68. Web.

- "Mars Global Surveyor | Mars Exploration Program." *NASA*. NASA, n.d. Web. 01 Mar. 2017. <http://mars.nasa.gov/programmissions/missions/past/globalsurveyor/>.

- Odstrcil, D. "Modeling 3-D Solar Wind Structure." *Advances in Space Research* 32.4 (2003): 497-506, DOI: 10.1016/S0273-1177(03)00332-6

- Poduval, B., and X. P. Zhao. "Validating Solar Wind Prediction Using The Current Sheet Source Surface Model." *ApJ The Astrophysical Journal* 782.2 (2014): n. pag. Web.

- Richardson, John D. "The Solar Wind in the Outer Heliosphere." *AIP Conference Proceedings* (2004): n. pag. Web.

- Xie, Hong, Leon Ofman, and Gareth Lawrence. (2004) "Cone Model for Halo CMEs: Application to Space Weather Forecasting." *Journal of Geophysical Research vol. 109, A03109,* DOI: 10.1029/2003JA010226

- Odstrčil, Dusan (2004). “Enlil: A Numerical Code for Solar Wind Disturbances.” http://ccmc.gsfc.nasa.gov/models/Code_description.pdf

- Usmanov,A.,V., A global nA Global Numerical 3-D MHD model of the solar wind, *Sol. Phys.,*145, 377-396, 1993